Coordinated planning of fast charging station and distribution network based on an improved flow capture location model

Coordinated Planning for Fast Charging Stations and Distribution Networks Based on an Improved Flow Capture Location Model

Shiqu Xiao, *Student Member*, *IEEE*, Xia Lei, *Member*, *IEEE*, *Member*, *CSEE*, Tao Huang, *Member*, *IEEE*, and Xiang Wang

***Abstract*—The increasing penetration of plug-in electric vehicles (PEVs) should lead to a significant reduction in greenhouse gas emissions. Nevertheless, the development of PEVs is limited by the lack of charging facilities, which is constrained by the coupled transportation-distribution network. This paper presents a stochastic bi-level model for the optimal allocation of fast charging stations (FCSs) and distribution network expansion planning (DNEP). First, a sequential capacitated flow-capturing location-allocation model (SCFCLM) is proposed at the lower level to optimize the allocation of FCSs on the transportation network. Monte-Carlo simulation (MCS) is utilized to estimate daily charging load requirements. Then, we propose an economic model for DNEP at the upper level, and the chance constrained method is employed to relax power flow constraints to address the uncertainties of loads. Numerical experiments are conducted to illustrate the proposed planning method. The influences of the flow capturing sequence and relaxed confidence level on the PEV charging load, FCS planning strategies and DNEP schemes are analyzed.**

***Index Terms*—Coordinated planning, fast charging station, flow-capturing model, plug-in electric vehicle, stochastic bi-level model.**

NOMENCLATURE

A. Sets

N^{T}	Set of transportation nodes.
E^{T}	Set of transportation links.
Q	Set of all Origin-Destination (OD) pairs.
Ω^{sub}	Set of substations.
Ω^{bus}	Set of distribution network buses.
Ω^{line}	Set of distribution network feeders.
$\Omega^{\mathrm{line,cons}}$	Set of feeders construction.
$\Omega^{\mathrm{line,up}}$	Set of feeders upgrade.

B. Parameters

e^q	Links on road network that belong to OD pair q.
D_q	The shortest distance between OD pair q, in km.
K	Number of FCSs in the planning area.
N^{PEV}	Number of PEVs exits on the road network.
p^{rated}	Rated power of fast charging piles, in kW.
c^{FCS}	Price of FCS providing fast charging service, in ¥/kWh.
c^{DS}	Unit cost of purchase power, in ¥/kWh.
η	Charging efficiency of charging piles.
r	Discount rate.
$T^{\mathrm{FCS/sub/line}}$	Service years of FCSs/substations/feeders.
c^{pile}	Unit cost of a charging pile, in ¥.
A	Required area of per charging pile, in m^2.
c_u^{land}	Land price of transportation node u, in ¥/m^2.
C^{other}	Other cost associated with FCS construction, in ¥.
$\lambda^{\mathrm{CSO/DSO}}$	Coefficient of operation and maintenance of CSO/DSO.
$C^{\mathrm{CSO/DSO,dc}}$	Cost of disposal facilities of CSO/DSO, in ¥.
$K^{\mathrm{FCS/sub/line,d}}$	The residual value at the end of $T^{\mathrm{FCS/sub/line}}$.
$n_u^{\mathrm{pile,max}}$	The maximum acceptable number of charging piles of node u.
$SOC^{\min/\max}$	State-of-Charge (SOC) threshold of PEVs.
c^{sub}	Upgrading cost per substation, in ¥.
c^{line}	Unit cost of construction and upgrade feeders, in ¥/km.
l_{ij}	Length of feeder ij, in km.
c^{E}	Unit cost of electricity supplied by upstream power system, in ¥/kWh.
c^{ENS}	Unit penalty cost of energy not supply, in ¥/kWh.
ω_{ij}	Annual failure rate of feeder ij.
$P_{i,t}^{\mathrm{LD}}, Q_{i,t}^{\mathrm{LD}}$	Active and reactive power of conventional load, respectively, in kW.
T^{fault}	Average duration of each failure, in h.
R_{ij}, X_{ij}	Resistance and reactance of feeder ij, respectively.
$P_{t,u}^{\mathrm{DS,max}}$	Power grid capacity limit at node u at time t, in kW.

Manuscript received February 28, 2021; revised May 20, 2021; accepted June 2, 2021. Date of online publication May 6, 2022; date of current version November 28, 2022. This work is supported in part by National Natural Science Foundation China (No. 51877181) and in part by the Innovation Fund of Postgraduate, Xihua University (No. YCJJ2020050).

S. Q. Xiao, X. Lei (corresponding author, email: snow_lei246@mail.xhu.edu.cn; ORCID: https://orcid.org/0000-0003-2975-145X), and X. Wang are with School of Electrical Engineering and Electronic Information, Xihua University, Chengdu 610039, China.

T. Huang is with Department Ingegneria Elettrica, Politecnico Di Torino, Torino 10129, Italy, and with School of Electrical Engineering and Electronic Information, Xihua University, Chengdu 610039, China.

DOI: 10.17775/CSEEJPES.2021.01470

C. Variables

χ_{e^q}	Binary variable for capturing flow on link e that belongs to OD pair q.
z_u	Binary variable for allocating an FCS at node u.
$N_{t,u}^{\mathrm{PEV}}$	Number of PEVs captured at node u at time t.
$N_{\tau,u}^{\mathrm{PEV,ch}}$	Number of PEVs being charged at node u at time τ.
$N_{\tau,u}^{\mathrm{PEV,in/out}}$	Number of PEVs plug in/pull out at node u at time τ, respectively.
$n_{u^s}^{\mathrm{pile}}$	Number of charging piles at transportation node u in the s-th order.
$n_{\tau,u}^{\mathrm{avil}}$	Number of available charging piles at node u at time τ.
x_i	Binary variable for substation upgrade.
y_{ij}	Binary variable for feeder construction decision.
$P_{i,t}^s, Q_{i,t}^s$	Active and reactive power imported from grid at bus i at time t, respectively, in kW.
$U_{i,t}$	Voltage magnitude of bus i at time t, in kV.
s_{ij}	Apparent power flows of feeder ij, in kVA.

I. Introduction

PLUG-IN electric vehicles are regarded as a promising tool in the fight to address climate change and energy shortages. Many countries have integrated developmental strategies for electric vehicle industries and corresponding infrastructures (e.g., electric vehicle charging stations, (EVCSs)) into their national energy planning. The "New Energy Vehicle Industry Development Plan (2021–2035)" issued by the Ministry of Industry and Information Technology of China in 2020 states that the sales of new energy vehicles, with PEVs as the mainstream, will account for 40% of vehicle sales by 2030 [1]. The requirement for increasing PEVs addresses the need to construct refined charging service networks. The development of EVCSs, as the connection between the transportation and electricity networks, is subject to the constraints of the two systems. Thus, the coordinated planning of the EVCS and distribution network is an essential technology for the fast development of PEVs.

It was proposed in [1] that the charging service network composed of destination (slow) charging posts and urgent (fast) charging stations would be constructed in China. The slow charging service network, mostly composed of distributed charging spots, serves auto users with enough charging time in private or public parking lots. Thus, its planning is limited primarily by the location of buildings is relatively simple. The urgent charging is needed by users making long trips exceeding the driving ranges of their PEVs [2]. The siting and sizing of FCSs are more complicated because: a) the spatial and temporal charging demands for FCSs are highly random and difficult to accurately forecast; b) the stochastic demands and acceptability of the distribution network need to be balanced. The optimal planning of FCSs has been studied by many researchers in recent years.

The Voronoi diagram has been widely used to plan charging service regions to determine the locations of FCSs, as well as to obtain the optimal sizing of FCSs combined with the traffic flow calculation [3] or the queuing theory [4]. However, the locations of FCSs determined by the Voronoi diagram may not meet the PEV charging demands, because it only reflects the static topology of transportation networks (TNs) but not the dynamic traffic flow and road capacities. The flow-capturing location-allocation model (FCLM), which locates facilities based on maximum traffic flow capturing, was proposed by M. John Hodgson in 1990 [5] and has attracted the attention of many researchers in recent years [6], [7]. The FCLM was improved by considering service range for both dedicated-trip demand and by-passing flow demand in [8]. M. Kuby and A. Lim presented a flow refueling location mode (FRLM) to locate refueling stations considering the driving range instead of the assumption that a flow would just pass one facility along its path in FCLM [9]. The FRLM has been extended to planning of EVCSs [10]–[14]. However, the selection sequence of traffic flow capturing nodes of FCLMs presented in the above references leads to capacity redundancy at the nodes with high captured flow and capacity shortages at the ones with low captured flow. The FCLM with a more reasonable selection sequence of flow capturing nodes should be formulated considering the capacity of FCSs.

The large-scale penetration of PEVs through FCSs brings shock loads into the distribution network so that the security and stability of the power grid would be weakened. A lot of research efforts have been devoted to the coordination of PEV integration and the operational requirements of the power grid in the planning phase to reduce the negative effects of the EVs on the grid. The co-planning strategy for multi-network coupled systems was widely accepted in the academic and industrial areas. In [6], a multi-objective collaborative planning method was employed to integrate power distribution and PEV charging systems. Before then, the planning of PEV charging systems and distribution systems were conducted separately by a two-stage planning method. According to the net present value (NPV), life cycle cost (LCC), and traffic capturing model, a multi-objective optimization was used in [4] to determine the sites and sizes of charging stations, which was constrained by coupled power-transportation systems. In [7], a multi-objective synergistic planning model was proposed to minimize the power losses and voltage deviations of the distribution system, as well as maximizing the EV flow. It is known that the non-unique optimal solutions for a multi-objective planning model would decrease its practicability. Meanwhile, the bi-level programming as an alternative effective method has also been used to coordinate the conflicting objectives of FCS planning costs and PEV users' benefits [15], [16], but seldom employed to deal with the coupled problems of the distribution network and transportation network. Reference [17] presented a dynamic bi-level model for distribution network planning considering different objectives of the distribution network operator and gridable parking lot owner. However, the TN features and the stochastic behavior of PEVs are ignored.

The uncertainties of charging load, which increases the operational risk to the power grid, must be considered in the planning model of the distribution network. Probability distribution, such as the Possion distribution, has been always

employed to describe the random charging load [6], [7], [18], [19], but it was pointed out in [20] that the estimation demands based on the prior probability might have considerable differences from the accurate distribution. In fact, the uncertainty programming instead of deterministic planning is an effective way to express the effect of random variables on systems and avoid the strict requirements for the quantity and quality of fundamental data [21]–[26]. Reference [23] provided a robust chance constraint model to express the uncertainties of the FCSs' service ability. In [24], the chance constraint programming was used to deal with the uncertainties of conventional loads and EV demands in the expansion planning of the distribution network and EV charging stations, satisfying the substation capacity within a specified confidence level. It is important that the relaxed level of constraints in the stochastic programming model of system planning should be properly selected to both reflect the impact of random demands and guarantee the security of the power system.

A stochastic bi-level planning framework for the planning of both FCS and the distribution network is proposed in this paper to integrate the power system and the transportation system. At the lower level, the optimal allocation of FCSs is determined for a charging station operator (CSO) based on the estimation of fast charging demands using an improved FCLM. At the upper level, the distribution network expansion planning (DNEP) model for a distribution system operator (DSO) is set up based on chance constraint programming depicting the uncertain load demands. The collaborative planning model ameliorates the performances of transportation and distribution networks within the two networks' constraints. The main contributions of this paper include:

- A sequential capacitated flow-capturing location model (SCFCLM) with an optimal capturing sequence is proposed to alleviate both the redundancies and the shortages of FCSs capacities. This model is presented by a two-stage planning method including maximization of the captured EV flow at stage 1 and an optimization model for maximizing profit and service efficiency of the CSO at stage 2.
- The benefit conflicts between the DSO and CSO in the planning of FCSs and distribution network are coordinated in a bi-level model, which balances the growing PEV charging demands and the security and economic performance of the power system.
- The chance constrained programming is used to express the impact of uncertainties related to charging demands on the node voltage and line power of the distribution network, whose limits are relaxed. The relaxed level is discussed to analyze its effect on the planning schemes.

The remainder of this paper is organized as follows: In Section II, the framework of bi-level planning is presented. In Section III, EV flow is optimally captured and FCSs are allocated by the SCFCLM. A chance constrained economic planning model for DSO is formulated in Section IV. Then, in Section V, the whole planning flowchart and solution algorithm is provided. The case study is shown in Section VI and Section VII concludes the paper.

II. The Framework of Bi-level Planning

The planning of the coupled transportation-distribution network refers to the interaction between them based on the planning of the two separate networks. It is assumed in this study that the transportation network planning scheme is provided by a charging service operator (CSO), and a distribution system operator (DSO) conducts DNEP. With the consideration of the economic output and service efficiency, the CSO aims to provide as much charging service as possible given the restrictions of the geographic conditions in the traffic network planning. The economic outcome and security of distribution network are considered by the DSO in DNEP based on the charging load peak. A bi-level programming model is utilized to coordinate the benefit conflicts between the CSO and DSO. It is obvious that the siting and sizing of FCSs are the common focuses in both the planning of the transportation network and the planning of the distribution network.

The decisions of upgrading feeders and substations are made based on aggregated loads composed of a conventional load and PEV charging load in the distribution network planning at the upper level. Considering the randomness of loads (especially the charging load), we employ a chance constrained programming model to relax the operational constraints of the power system. The feasible set of FCS locations and capacities satisfying the operational constraints of the power system is sent to the lower level. At the lower level, a novel SCFCLM is proposed to optimize the sites and sizes of FCSs from the feasible set in the transportation network planning, which maximizes the NPV and efficiency of FCSs based on the maximum captured EV flow. According to the planning scheme of FCSs, the charging demand profile simulated by MCS is sent to the upper level.

III. The Lower Level: The SCFCLM For CSO

In this section, the SCFCLM is described in two stages: 1) maximizing the captured EV flow to obtain the candidate nodes set $\boldsymbol{z}$ for locating FCSs; 2) maximizing the profit and service efficiency of the CSO to determine the optimal capturing sequence of nodes in set $\boldsymbol{z}$ and the sites and sizes of FCSs. Charging demand estimation is simulated by MCS based on the fitting distribution of charging behavior of PEVs that is obtained from the practical data.

A. Flow Capturing Location Model

$G^{\mathrm{T}}(N^{\mathrm{T}}, E^{\mathrm{T}})$ is used to represent an urban transportation network, where N^{T} is the set of transportation nodes and E^{T} is the set of links connecting these nodes, which represent critical road interactions, main areas, or locations with high traffic [25]. PEV drivers are assumed to make their trips according to a matrix of OD pairs represented by Q. A list of connected m links $\{e_1^q, e_2^q, \cdots, e_m^q\}$ connects origin o ($o \in N^{\mathrm{T}}$) and destination d ($d \in N^{\mathrm{T}}$), that is, the OD pair q. The objective, which determines the locations of FCSs by capturing the maximum EV flow, can be expressed as:

$$\max_{z} f = \sum_{t} \sum_{q \in Q} \mathrm{flow}_{t,\mathrm{e}^q} \chi_{\mathrm{e}^q} \tag{1}$$

subject to:

$$z_u \geq \chi_{\mathrm{e}^q},\ \forall q \in Q, u \in N^{\mathrm{D2T}} \tag{2}$$

$$\sum_{u \in N^{\mathrm{D2T}}} z_u = K \tag{3}$$

where N^{D2T} is a feasible set of FCSs locations obtained from the calculation at the upper level; $\mathrm{flow}_{t,\mathrm{e}^q}$ represents the time-varying traffic flow of EVs over the link e that belongs to the OD pair q at time t, and is calculated by the gravity model as:

$$\mathrm{flow}_{t,q} = 1.5\frac{w^{\mathrm{o}}_{t,u_1} w^{\mathrm{d}}_{t,u_2}}{D_q^2},\ \forall u_1 \neq u_2 \in N^{\mathrm{T}}, t \in [1,24] \tag{4}$$

where $w^{\mathrm{o}}_{t,u}$ and $w^{\mathrm{d}}_{t,u}$ are the weights of node u as an origin and a destination, respectively. $w^{\mathrm{o}}_{t,u}$, $w^{\mathrm{d}}_{t,u}$ obtained from the traffic survey data are nodal attractions to EVs, which consider multiple factors, such as road capacity, average speed to vehicles, traffic congestion, *et al*. D_q is calculated by using the Floyd method. The impact of congestion on EVs and other vehicles could be modeled by regarding them as congestion takers [27].

The objective in (1) is to maximize the capturing EV flow during a typical day. Equation (2) means the flow on link e^q can be captured only if there is an FCS that exists at the node u, which is within the OD pair q. Equation (3) ensures that K FCSs are located in the planning area.

B. Charging Demand Estimation

The time-varying charging demand needs to be estimated on the capturing flow. Since [28] proved that the calculated traffic flow was proportional to the practical traffic, the number of PEVs that are captured at node u at time t can be calculated by:

$$N^{\mathrm{PEV}}_{t,u} = N^{\mathrm{PEV}}\frac{\mathrm{flow}_{t,u}}{\sum_u^K \mathrm{flow}_{t,u}},\ \forall t \in [1,24] \tag{5}$$

where $\mathrm{flow}_{t,u}$ is the EV flow captured at node u at time t.

In our study, only the PEVs with fast charging demand are considered. The plug-in time and charging duration are necessary information for charging demand estimation because some PEVs leave without a full SOC. The plug-in time of PEVs during a day follows the Gauss Distribution as (6), and their charging duration follows the Chi-square Distribution as (7), as suggested in [20] and [29]. It is assumed that a day is divided into four time periods with different probability distribution parameters: (0, 8], (8, 15], (15, 19], (19, 24] (in hours). The charging behavior of each PEV is sampled through MCS, which provides acceptable computational flexibility and efficiency.

$$f(x|\sigma_t,\mu_t) = \frac{1}{\sqrt{2\pi}\sigma_t}\mathrm{e}^{-\frac{(x-\mu_t)}{2\sigma_t^2}} \tag{6}$$

$$C(x|n_t) = \frac{1}{2^{n_t/2}\Gamma(n_t/2)}x^{\frac{n_t}{2}-1}\mathrm{e}^{-x/2} \tag{7}$$

Because the time duration of fast charging is usually from 15 to 120 minutes, the calculation interval of charging power is assumed to be 15 minutes. Thus, a day is divided into 96 calculation periods, each of which is presented by τ ($\tau = 1, 2, \cdots, 96$). The number of PEVs charged at the transportation node u at time τ can be calculated as:

$$N^{\mathrm{PEV,ch}}_{\tau,u} = N^{\mathrm{PEV,ch}}_{\tau-1,u} + N^{\mathrm{PEV,in}}_{\tau,u} + N^{\mathrm{PEV,out}}_{\tau,u} \tag{8}$$

The charging power of FCSs at node u at time τ is:

$$P^{\mathrm{FCS}}_{\tau,u} = p^{\mathrm{rated}} N^{\mathrm{PEV,ch}}_{\tau,u} \tag{9}$$

It should be mentioned that the SOC and charging state of the PEVs during the last calculation period of a day are kept to the beginning period of the next day. This ensures the continuity of the simulated SOC of a PEV. The simulation for N^{PEV} PEVs in the 96 time periods is implemented.

C. Sequential Capacitated Model

1) Analysis of capturing sequences

We observe that the sum of capturing flow is fixed for a settled candidate node set z, while the capturing flow of each candidate node will be affected by the selected sequences. A simple example is shown in Fig. 1. $z = \{A, B, C\}$ is supposed to be a candidate nodes set. The links in different colors represent the EV flow on different OD pairs and the thickness of the links represents the EV flow.

Capturing sequences and capturing flow in FCLM ($\boldsymbol{s} = (\mathrm{A}^1 \rightarrow \mathrm{B}^2 \rightarrow \mathrm{C}^3)$) and an arbitrary one ($\boldsymbol{s} = (\mathrm{B}^1 \rightarrow \mathrm{C}^2 \rightarrow \mathrm{A}^3)$) are depicted in Fig. 1(a) and Fig. 1(b), respectively. The same uncaptured flow after the terminal capturing with different flow at each node in the two cases can be seen in Fig. 1. Too much flow is captured at the front capturing nodes (such as node A) and too little flow is captured at the last capturing nodes (such as node C) in the FCLM as shown in Fig. 1(a). The charging demand will be overestimated and numerous charging piles will be installed at node A, while fewer piles will be installed at node C due to the underestimation of charging demand. The current maximum flow captured at each sequential node in FCLM may cause two disadvantages:

- Capacity redundancy may emerge from the large-scale FCSs at high-capturing flow nodes in off-peak periods, which results in the low utilization of FCSs.
- Some PEVs that should be charged may be lost in the small-scale FCSs with inadequate charging resources. Capacity shortage of FCSs causes loss of profit or larger opportunity costs.

2) Optimization Model

To overcome the above-mentioned disadvantages, the second stage of SCFCLM is to select the optimal capturing sequence in the candidate set z obtained in stage 1, and then determine the sizes of the FCSs. The objectives considering the NPV and utilization efficiency of FCSs are formulated in (10) and (11), respectively.

$$\max F_1^{\mathrm{CSO}} = R^{\mathrm{E}} - C^{\mathrm{Cons}} - C^{\mathrm{FCS,O\&M}} - C^{\mathrm{D,FCS}} \tag{10}$$

$$\max F_2^{\mathrm{CSO}} = K/\sum_{u=1}^{K}\left(P_u^{\mathrm{FCS,max}} - \overline{P}_u^{\mathrm{FCS}}\right)^2 \tag{11}$$

Equation (11) is a reciprocal of variance of peak load for the FCSs, which represents the impact of capacity redundancy and

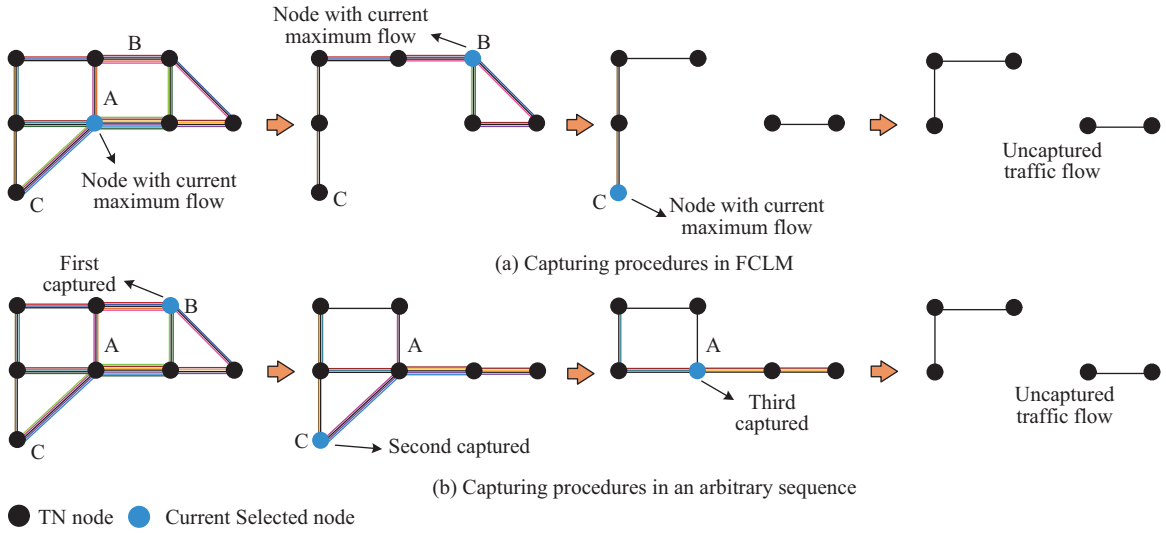

Fig. 1. Capturing flow with different capturing sequences.

insufficiency on the operational efficiency of the FCSs. The income of providing charging services (R^{E}), construction costs (C^{Cons}), operation and maintenance costs ($C^{\mathrm{FCS,O\&M}}$), and disposal costs ($C^{\mathrm{FCS,D}}$) are calculated in (12)–(15), respectively. To simplify the problem, the operation and maintenance costs are proportional to construction costs as shown in (14). d^{FCS} is the depreciation rate of an FCS calculated by (16).

$$R^{\mathrm{E}} = 365 \sum_{\tau} \sum_{u^s \in \boldsymbol{s}} P_{\tau,u}^{\mathrm{FCS}} \left(\eta c^{\mathrm{FCS}} - c^{\mathrm{DS}}\right) \tag{12}$$

$$C^{\mathrm{Cons}} = \frac{r(1+r)^{T^{\mathrm{FCS}}}}{(1+r)^{T^{\mathrm{FCS}}} - 1} \cdot \sum_{u^s \in \boldsymbol{s}} z_u \left[\left(c^{\mathrm{pile}} + A c_u^{\mathrm{land}}\right) n_{u^s}^{\mathrm{pile}} + C^{\mathrm{other}}\right] \tag{13}$$

$$C^{\mathrm{FCS,O\&M}} = \lambda^{\mathrm{CSO}} C^{\mathrm{Cons}} \tag{14}$$

$$C^{\mathrm{FCS,D}} = C^{\mathrm{CSO,dc}} - C^{\mathrm{Cons}} \left(1 - d^{\mathrm{FCS}}\right)^{T^{\mathrm{FCS}}} \tag{15}$$

$$d^{\mathrm{FCS}} = 1 - T^{\mathrm{FCS}} \sqrt{K^{\mathrm{FCS,d}} / C^{\mathrm{Cons}}} \tag{16}$$

Subject to:

$$n_{\tau,u}^{\mathrm{avil}} = n_u^{\mathrm{pile}} - N_{\tau,u}^{\mathrm{PEV,ch}} \tag{17}$$

$$N_{\tau,u}^{\mathrm{PEV,ch}} \le n_u^{\mathrm{pile}} \le n_u^{\mathrm{pile,max}} \tag{18}$$

$$P_{\tau,u}^{\mathrm{FCS,ch}} \le \min\left(p^{\mathrm{rated}} n_{u^s}^{\mathrm{pile}}, P_{t,u}^{\mathrm{DS,max}}\right), (\tau \in t) \tag{19}$$

$$SoC^{\min} \le SoC_{\tau,ev} \le SoC^{\max} \tag{20}$$

The number of available charging piles is limited by (17). Equation (18) provides the constraints of the installed charging piles at node u and charging vehicles at node u at time τ. The charging power is limited to the availability of the FCS or the grid secure capacity at node u at time τ as formulated in (19). Equation (20) is the constraint for the SOC of the PEV's battery.

It should be noted that in some cases, especially when the capturing sequence approaches to the end, there might be some links connected to only one node, resulting to multiple optima in terms of capturing sequences.

3) Normalization of Objectives

Two objectives with different dimensions as (10) and (11) are normalized as (21).

$$F_i^{\mathrm{CSO,norm}} = \frac{F_i^{\mathrm{CSO}} - F_i^{\mathrm{CSO,min}}}{F_i^{\mathrm{CSO,max}} - F_i^{\mathrm{CSO,min}}} \quad i = 1, 2 \tag{21}$$

where, $F_i^{\mathrm{CSO,min/max}}$ are minimum/maximum values of the i-th objective function in stage 2. The value of function $F_i^{\mathrm{CSO,norm}}$ lies in range [0, 1]. The final solution selected by the objective of stage 2 can be expressed as:

$$F^{\mathrm{CSO}} = \max \prod_{i=1}^{2} F_i^{\mathrm{CSO,norm}} \tag{22}$$

IV. The Upper Level: DNEP Model

The expansion planning for the distribution power system considering the uncertainties of charging power is carried out by the DSO based on the FCS planning scheme and charging demand in a typical day obtained from CSO.

A. Objective Function

The DNEP objective is to minimize annual investment, considering the life-cycle costs of devices.

$$\min C^{\mathrm{DSO}} = C^{\mathrm{sub}} + C^{\mathrm{line}} + C^{\mathrm{DN,O\&M}} + C^{\mathrm{D,DN}} + C^{\mathrm{loss}} + C^{\mathrm{ENS}} \tag{23}$$

$$C^{\mathrm{sub}} = \frac{r(r+1)^{T^{\mathrm{sub}}}}{(1+r)^{T^{\mathrm{sub}}} - 1} \sum_{i \in \Omega^{\mathrm{sub}}} x_i c^{\mathrm{sub}} \tag{24}$$

$$C^{\mathrm{line}} = \frac{r(r+1)^{T^{\mathrm{line}}}}{(r+1)^{T^{\mathrm{line}}} - 1} \sum_{ij \in (\Omega^{\mathrm{line,cons}} \cup \Omega^{\mathrm{line,up}})} y_{ij} c^{\mathrm{line}} l_{ij} \tag{25}$$

$$C^{\mathrm{DN,O\&M}} = \lambda^{\mathrm{DNO}} \left(C^{\mathrm{sub}} + C^{\mathrm{line}}\right) \tag{26}$$

$$C^{\mathrm{DN,D}} = C^{\mathrm{DSO,dc}} - C^{\mathrm{sub}} \left(1 - d^{\mathrm{sub}}\right)^{T^{\mathrm{sub}}} - C^{\mathrm{line}} \left(1 - d^{\mathrm{line}}\right)^{T^{\mathrm{line}}} \tag{27}$$

$$d^{\mathrm{sub/line}} = 1 - T^{\mathrm{sub/line}} \sqrt{K^{\mathrm{sub/line,d}} / C^{\mathrm{sub/line}}} \tag{28}$$

$$C^{\mathrm{loss}} = 365 c^{\mathrm{E}} \sum_{ij \in \Omega^{\mathrm{line}}} \sum_{t} P_{ij}^{\mathrm{loss}} R_{ij} \tag{29}$$

$$C^{\mathrm{ENS}} = 365 c^{\mathrm{ENS}} \sum_{t} \sum_{ij \in \Omega^{\mathrm{line}}} \omega_{ij} \cdot \left(\sum_{j \in \Omega^{\mathrm{bus}}} \left(P_j^{\mathrm{LD,max}} + P_j^{\mathrm{FCS,max}} \right) T^{\mathrm{fault}} \right) \tag{30}$$

where the costs of annual investment for substations (C^{sub}) and feeders (C^{line}) based on their life-cycle costs are expressed by (24)–(25). The operation and maintenance ($C^{\mathrm{DN,O\&M}}$) costs and disposal costs ($C^{\mathrm{DN,D}}$) are evaluated as given in (26)–(27), respectively. $d^{\mathrm{sub/line}}$ is the depreciation rate of substations or feeders calculated by (28). The binary variables x_i, y_{ij} represent whether or not to make the investment decisions. The costs of active power loss (C^{loss}) and energy not supplied (C^{ENS}) are determined by (29) and (30), respectively. C^{ENS} is estimated without taking the DGs and battery discharging of PEVs into account.

B. Constraints

The constraints of the distribution system include the power flow constraints and the logical constraints of the radial network. The power flow constraints are formulated in (31)–(35). Equations (31)–(32) correspond to Kirchhoff's laws and represent the active and reactive power balances at each distribution network bus. Capacity limits for substations and feeders are expressed by (33) and (34), respectively. Equation (35) is the constraint of the bus voltage magnitude. Equation (36) represents the redundant construction of feeders.

$$P_{i,t}^{s} = P_{i,t}^{\mathrm{LD}} + P_{i,t}^{\mathrm{FCS}} + U_{i,t} \sum_{j \in i} U_{j,i} R_{ij}, \ \forall i \in \Omega^{\mathrm{bus}} \tag{31}$$

$$Q_{i,t}^{s} = Q_{i,t}^{\mathrm{LD}} + U_{i,t} \sum_{j \in i} U_{j,t} X_{ij}, \ \forall i \in \Omega^{\mathrm{bus}} \tag{32}$$

$$S_{i,t}^{\mathrm{sub}} \le \overline{S}_i^{\mathrm{sub}}, \ \forall i \in \Omega^{\mathrm{bus}} \tag{33}$$

$$s_{ij}^2 \le \overline{s}_{ij}^2, \ \forall ij \in \Omega^{\mathrm{line}} \tag{34}$$

$$U_i \le U_{i,t} \le \overline{U}_i, \ \forall i \in \Omega^{\mathrm{bus}}, t \in [1,24] \tag{35}$$

$$y_{ij} \le 1, \ \forall ij \in \left\{ \Omega^{\mathrm{line,Cons}} \cup \Omega^{\mathrm{line,up}} \right\} \tag{36}$$

Equations (37)–(42) ensure the radiality and connectivity of the distribution network. Here, based on a spanning tree corresponding to the distribution network [30], we introduce two binary variables δ_{ij} and φ_{ij}, where δ_{ij} is the connection state indicator of the feeder ij, $\delta_{ij} = 1$, if ij is connected, $\delta_{ij} = 0$, otherwise; φ_{ij} is a binary indicator of feeder ij, $\varphi_{ij} = 1$, if bus i is the parent node of bus j, $\varphi_{ij} = 0$, otherwise. In the spanning tree, every bus except the roots (substations) has one parent. These characteristics can be expressed by (38)–(42). Equation (38) indicates that a feeder ij is connected if either bus j is the parent node of bus i, or i is the parent node of j. Equations (39) and (40) indicate that every bus has exactly one parent node, while substation nodes have no parent node. Equations (41) and (42) imply that φ_{ij} and δ_{ij} are binary variables.

$$\sum_{ij \in \Omega^{\mathrm{line}}} \delta_{ij} = n^{\mathrm{bus}} - n^{\mathrm{sub}} \tag{37}$$

$$\varphi_{ij} + \varphi_{ji} = \delta_{ij}, \ ij \in \Omega^{\mathrm{line}} \tag{38}$$

$$\sum_{j \in \Omega_i} \varphi_{ji} = 1, \ \forall i \in \Omega^{\mathrm{bus}} \tag{39}$$

$$\varphi_{0j} = 0, \ \forall j \in \Omega^{\mathrm{sub}} \tag{40}$$

$$\varphi_{ij} \in \{0,1\}, \ \forall i \in \Omega^{\mathrm{bus}}, j \in \Omega_i \tag{41}$$

$$\delta_{ij} \in \{0,1\}, \ ij \in \Omega^{\mathrm{line}} \tag{42}$$

where n^{bus} and n^{sub} are the number of buses and substations, respectively. Ω_i is the set of nodes connected to node i by a feeder.

C. Chance Constraints for DNEP

The operational constraints in the planning of the grid are usually limited by the maximum load. However, we cannot simply obtain the maximum load by adding the peak value of each type of load as they do not necessarily appear at the same time (i.e., their simultaneous rate). So the expensive equipment configuration for strict security requirements of power system like equations (34)–(35) may not be necessary. The chance constrained programming method can express that the decisions are made before the realization of the random variables forecast when there are random variables in the constraints of the optimization model. Chance constraints in (43) and (44) are used to satisfy the limits of the feeder capacity in (34) and voltage in (35) within the determined confidence levels (ε_1 and ε_2) considering the randomness of the charging demand and conventional load and their simultaneous rate. Furthermore, the confidence level can also define the expected overall system security set by the policy decision makers.

$$\mathrm{Prob}\left\{ s_{ij,t}^2 \le \overline{s}_{ij}^2 \right\} \ge \varepsilon_1, \ \forall ij \in \Omega^{\mathrm{line}} \tag{43}$$

$$\mathrm{Prob}\left\{ U_j \le U_{j,t} \le \overline{U}_j \right\} \ge \varepsilon_2, \ \forall j \in \Omega^{\mathrm{bus}} \tag{44}$$

where

$$\begin{aligned} s_{ij,t}^2 &= p_{ij,t}^2 + q_{ij,t}^2 = \left(U_{i,t} U_{j,t} R_{ij}\right)^2 + \left(U_{j,t} U_{j,t} X_{ij}\right)^2 \\ &= \left(X_{ij}^2 + R_{ij}^2\right) \left(U_{i,t}^4 - 2U_{i,t}^2 \left[\left(P_{i,t}^{\mathrm{LD}} + P_{i,t}^{\mathrm{FCS}}\right) R_{ij} + Q_{i,t}^{\mathrm{LD}} X_{ij} \right] + \left[\left(P_{i,t}^{\mathrm{LD}} + P_{i,t}^{\mathrm{FCS}}\right)^2 + \left(Q_{i,t}^{\mathrm{LD}}\right)^2 \right] \cdot \left(R_{ij}^2 + X_{ij}^2\right) \right) \end{aligned} \tag{45}$$

$$\begin{aligned} U_{j,t} &= \sqrt{\left(U_{i,t} - \frac{P_{i,t} R_{ij} + Q_{i,t} X_{ij}}{U_{i,t}} \right)^2 + \left(\frac{P_{i,t} X_{ij} - Q_{i,t} R_{ij}}{U_{i,t}} \right)^2} \\ &= \sqrt{\frac{U_{i,t}^2 - 2\left[\left(P_{i,t}^{\mathrm{LD}} + P_{i,t}^{\mathrm{FCS}}\right) R_{ij} + Q_{i,t}^{\mathrm{LD}} X_{ij} \right] + \left[\left(P_{i,t}^{\mathrm{LD}} + P_{i,t}^{\mathrm{FCS}}\right)^2 + \left(Q_{i,t}^{\mathrm{LD}}\right)^2 \right] \cdot \left(R_{ij}^2 + X_{ij}^2\right)}{U_{i,t}^2}} \end{aligned} \tag{46}$$

V. Solution Methodology of the Bi-Level Stochastic Programming Model

The proposed bi-level planning problem coupled distribution and transportation networks is a largescale mixed integer

nonlinear problem (MINLP), which is hard to be solved and converge through traditional optimization methods [31]. Intelligent algorithms, such as the genetic algorithm (GA), show a better performance when the time for solving the model is not affected by the complexity of the problem. The disadvantage of GA that it is easy to fall into the local optimal solution which can be prevented at the cost of calculation time or by the improved genetic procedures. In our study, an improved genetic algorithm (IGA) [32] and GA are utilized to optimize the DNEP and FCS allocations, respectively.

The cross iterations have been carried out between the upper level and the lower level until the predefined maximum number of iterations is reached or there is little change in the optimal results. The initial optimization is made at the upper level without considering the charging load. The feasible nodes set for FCS configuration in the most economical DNEP scheme obtained at the upper level is sent to the lower level. Afterwards, the optimal sites and sizes of FCSs in the feasible nodes set are determined by the SCFCLM at the lower level and the estimated charging demand is returned to the upper level to adjust the DNEP strategies. The overall pseudo code of solving the proposed stochastic bi-level problem is detailed in Algorithm 1.

VI. Case Studies and Discussions

A. Case Overview and Parameter Settings

A 25-node urban transportation network [5] coupled with a 54-bus 10 kV distribution network depicted in Fig. 2 is used to test the proposed stochastic bi-level planning method. The "bus-node" coupling relationship is noted in Table I. According to Eq. (4), the heatmap of the OD matrix representing the EV flow at time $t = 7$ is presented in Fig. 3. It can be observed

Algorithm 1: Framework of the Bi-Level Planning Problem

Input the initial information of TN and DN
Set the number of FCSs K and the number of iterations $iter^{\max}$.
while $iter \le iter^{\max}$ *or* $\begin{cases} C^{\mathrm{DSO}}_{iter} - C^{\mathrm{DSO}}_{iter-1} > 10^{-5} \\ F^{\mathrm{CSO}}_{iter} - F^{\mathrm{CSO}}_{iter-1} > 10^{-5} \end{cases}$ **do**
  Upper Level Optimization
  if *iter* $\neq 1$ **then**
    Receive charging demand of CSO $\left\{P^{\mathrm{FCS}}_{\tau,u}\right\}$ from the lower level.
  end
  Initialize n^{DSO} individuals for DNEP and calculate their fitness (23).
  while $iter^{\mathrm{DSO}} \le iter^{\mathrm{DSO,max}}$ **do**
    Selection, cross, mutation, update next generation.
    Calculate fitness (23) for every individual.
    Update the best known individual.
    $iter^{\mathrm{DSO}} = iter^{\mathrm{DSO}} + 1$
  end
  Select the FCS feasible set N^{D2T} from the best DNEP individual and send it to the lower level.
  Lower Level Optimization
  Receive FCS feasible set N^{D2T} from the upper level.
  Stage 1: generate $\left|N^{\mathrm{D2T}}\right|!/\left(\left|N^{\mathrm{D2T}}\right| - K - 1\right)$ individuals for flow capturing.
  for $i = 1$ *to* $\left|N^{\mathrm{D2T}}\right|!/\left(\left|N^{\mathrm{D2T}}\right| - K - 1\right)$ **do**
    Calculate EV flow captured by each individual.
  end
  Select the individual $\boldsymbol{z}$ with the maximum captured flow.
  Stage 2: Initialize n^{CSO} individuals based on $\boldsymbol{z}$, that is, initialize the capturing sequences $\boldsymbol{s}$ of all the K FCSs, and calculate their fitness (10)–(11).
  while $iter^{\mathrm{CSO}} \le iter^{\mathrm{CSO,max}}$ **do**
    Selection, cross, mutation, update next generation.
    Decide each PEV's behavior according to (6)–(7) using MCS and estimate the charging demand of each FCS (8)–(9).
    Decide the optimal number of piles in each FCS according to the charging demand $\left\{P^{\mathrm{FCS}}_{\tau,u}\right\}$.
    Calculate the F^{CSO} (22) for every individual.
    Update the best known individual.
    $iter^{\mathrm{CSO}} = iter^{\mathrm{CSO}} + 1$
  end
  Select the charging demand profile $\left\{P^{\mathrm{FCS}}_{\tau,u}\right\}$ of the best individual and send it to the upper level.
end
Output the FCS siting and sizing strategy, the DNEP strategy, and the optimal fitness of the two levels.

TABLE I
COUPLED NODE SET OF TWO NETWORKS

Bus ID	01	04	09	12	13	19	27	28	30	35	40	41	46	50	54
Node ID	05	07	04	14	22	02	12	16	08	11	13	17	19	25	09
Land Price (¥/m^2)	13500	20100	13500	28350	13500	13500	13500	13500	28350	20100	7950	13500	28350	7950	13500

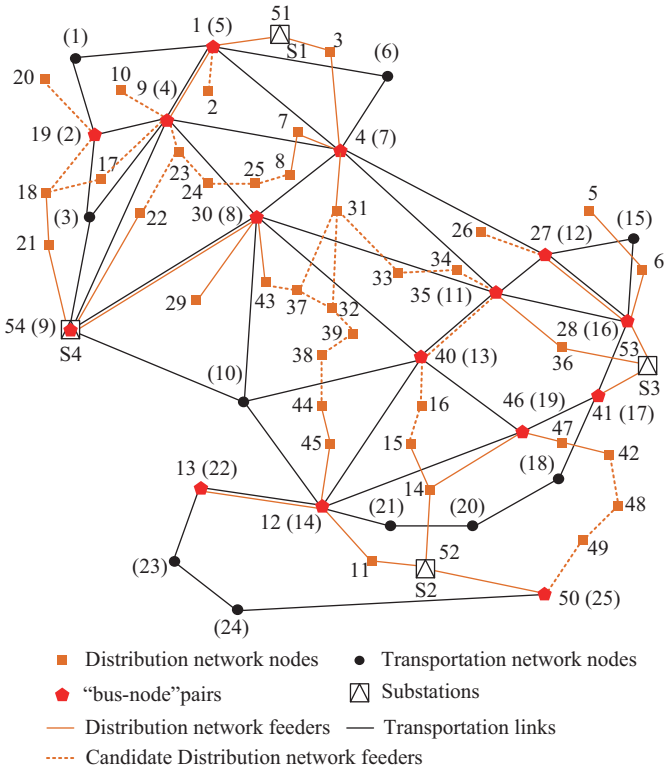

Fig. 2. A coupled transportation-distribution system.

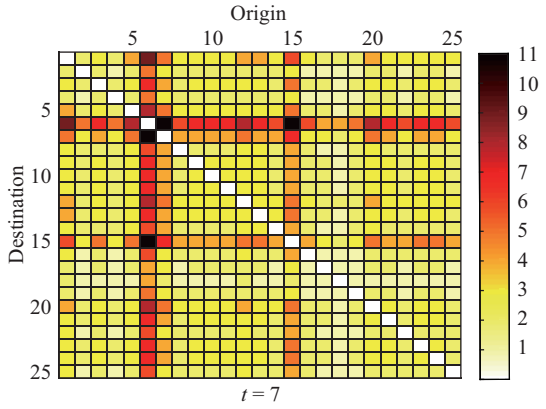

Fig. 3. OD matrix at time t ($t = 7$).

that during the morning rush hour, the links associated with nodes 6 or 15 have plenty of EV flows passing by. We assume the number of PEVs entering and exiting the planned area is in a dynamic equilibrium.

6 FCSs (that is $K = 6$) are assumed to be allocated for 2,000 PEVs ($N^{\mathrm{PEV}} = 2000$) in the area. The voltage constraints are $\underline{U}_i = 0.93$ and $\overline{U}_i = 1.07$, and the feeder current limits are set at their rated capacities. c^{sub} is 6×10^6 ¥ per substation. The parameters μ, σ, and n in (6)–(7) describing charging behavior of PEV drivers are divided into four time periods according to the probability distribution obtained from the real data in Shenzhen [20], as shown in Table II. Other parameters of the bi-level programming are shown in Table III. For the GA and IGA used to solve the bi-level model, the number of decision variables are 64 (decisions of all candidate feeders and substations) in the GA and $2 \times K$ (the sites and sizes of all the FCSs) in the IGA, population size is 50, the crossover probability is 0.85, the mutation probability is 0.05, and the number of iterations is 100. We use MATLAB to solve the optimal problem and the forward-backward sweep method to calculate the power flow on a computer with a quadcore Intel Core i3 processor and 8 GB memory.

TABLE II
PARAMETERS OF CHARGING BEHAVIOR DISTRIBUTION

Time (h)	μ_t	σ_t	n_t
(0, 8]	3.93	1.86	0.35
(8, 15]	11.94	1.36	0.3
(15, 19]	16.98	0.90	0.33
(19, 24]	21.56	0.98	0.27

TABLE III
PLANNING PARAMETERS OF BI-LEVEL PROGRAMMING

Parameter	Value	Parameter	Value
$T^{\mathrm{sub/l}}$	20 years	c^{E}	0.55 ¥/kWh
$\lambda^{\mathrm{CSO/DSO}}$	0.1	η	90%
N^{PEV}	2000	r	0.08
p^{rated}	44 kW [6]	T^{FCS}	10 years
c^{FCS}	2 ¥/kWh	c^{DS}	0.5 ¥/kWh
c^{pile}	88000 ¥	C^{other}	40000 ¥
A	20 m^2	c^{ENS}	0.15 ¥/kWh

B. Deterministic Planning Results and Analysis

To demonstrate the advantages of the proposed SCFCLM, the following four cases are compared.

Case 1: EV flow captured by SCFCLM; the objective of CSO includes the NPV and operational efficiency.

Case 2: EV flow captured by FCLM; the objective of CSO includes the NPV and operational efficiency.

Case 3: EV flow captured by SCFCLM; the objective of CSO only includes the NPV of FCSs.

Case 4: EV flow captured by SCFCLM; the objective of CSO only includes operational efficiency.

The planning topology results of the 4 cases are depicted in Fig. 4. The updating feeders in the four cases are presented by blue, purple, green and pink lines, respectively. The reinforced substation locations in the four cases are shown as different color signs. The pile numbers of each FCS in the cases are labeled near the EV pictures. The charging demand curves in all cases are depicted in Fig. 5. The planning results of all cases are demonstrated in Table IV and Fig. 6.

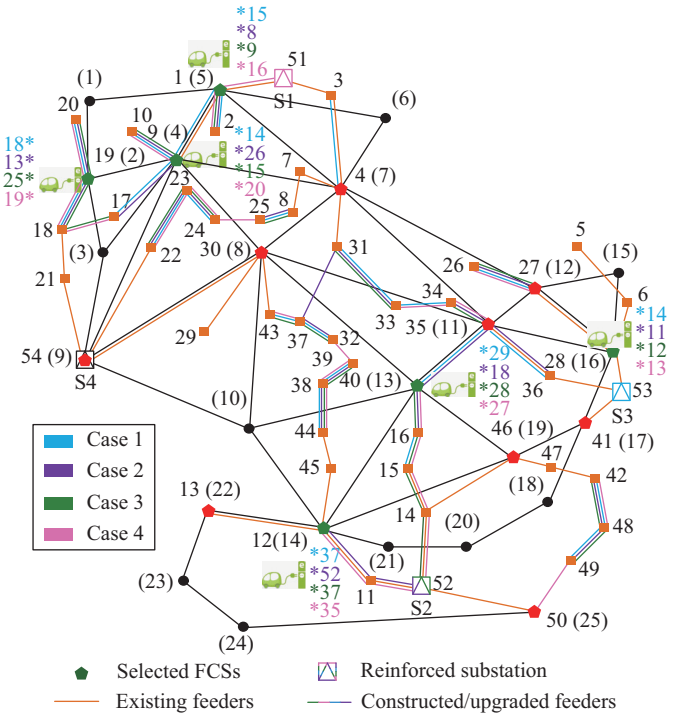

Fig. 4. Planning results of cases 1–4.

TABLE IV
PLANNING RESULTS OF ALL CASES

Case	FCS Planning Strategy		Total Num.	Average Service Ability
1	Sequence $\boldsymbol{s}$	(13→2→5→16→4→14)	126	9.91%
	Pile Num.	(29, 18, 15, 14, 14, 36)		
2	Sequence $\boldsymbol{s}$	(14→4→13→2→16→5)	128	5.42%
	Pile Num.	(52, 26, 18, 13, 11, 8)		
3	Sequence $\boldsymbol{s}$	(13→2→4→16→5→14)	126	7.18%
	Pile Num.	(28, 25, 15, 12, 9, 37)		
4	Sequence $\boldsymbol{s}$	(13→4→2→5→16→14)	130	11.08%
	Pile Num.	(27, 20, 19, 16, 13, 35)		
5	Sequence $\boldsymbol{s}$	(13→2→5→16→14→4)	138	8.76%
	Pile Num.	(21, 27, 10, 20, 43, 17)		
6	Sequence $\boldsymbol{s}$	(4→13→16→14→2→5)	142	7.92%
	Pile Num.	(21, 24, 23, 42, 19, 13)		

The same nodes are selected in the four cases as shown in Table IV and a 76.37% average flow is captured during a day, which verifies that the effectiveness of SCFCLM is consistent with FCLM (case 2). Different capturing sequences result in the differences of capturing flow at each node, and further impact the number of charging piles allocated at each FCS and its operational efficiency. We take node 14 (bus 12) as an example due to its significance in TN to compare the results of SCFCLM and FCLM in case 1 and case 2, respectively. In case 2, as shown in Table IV and the green curve in Fig. 5(b), node 14 is the first selected one and captures the maximum flow, where the FCS has the largest capacity (52 piles) and the highest charging peak (2.488 MW) in all cases. Moreover, the capacity and peak of node 14 are much larger than those of the other nodes. The service ability (SA) [3] of node 14 (that is, the ratio of the charging PEVs to the number of piles in the valley hour) is only 4.52% and the average SA of all FCSs is 5.42%, which means that the planning strategy by FCLM generates the greater redundancy of FCS capacity during off-peak charging periods. Meanwhile, the FCS which allocated 8 piles at node 5 cannot meet the incremental PEV penetration and will cause the deficiency of SA due to its small-scale. Compared with case 2, the FCS at node 14 in case 1 based on the SCFCLM has the better performance with a charging peak 1.584 MW and SA 11.11%. In addition, since the charging load of high capturing nodes in case 1 is partially transferred to the other nodes, it is in favor of the FCS future development. We observe that capturing sequences impact not only on the planning strategy of FCSs, but also on the DNEP. With the help of SCFCLM, the total investment of DNEP in case 1 is 8.865 M¥ and less than 9.007 M¥ in case 2. Since the DSO in case 1 faces fewer risks of peak load, it will reduce the investment for grid security.

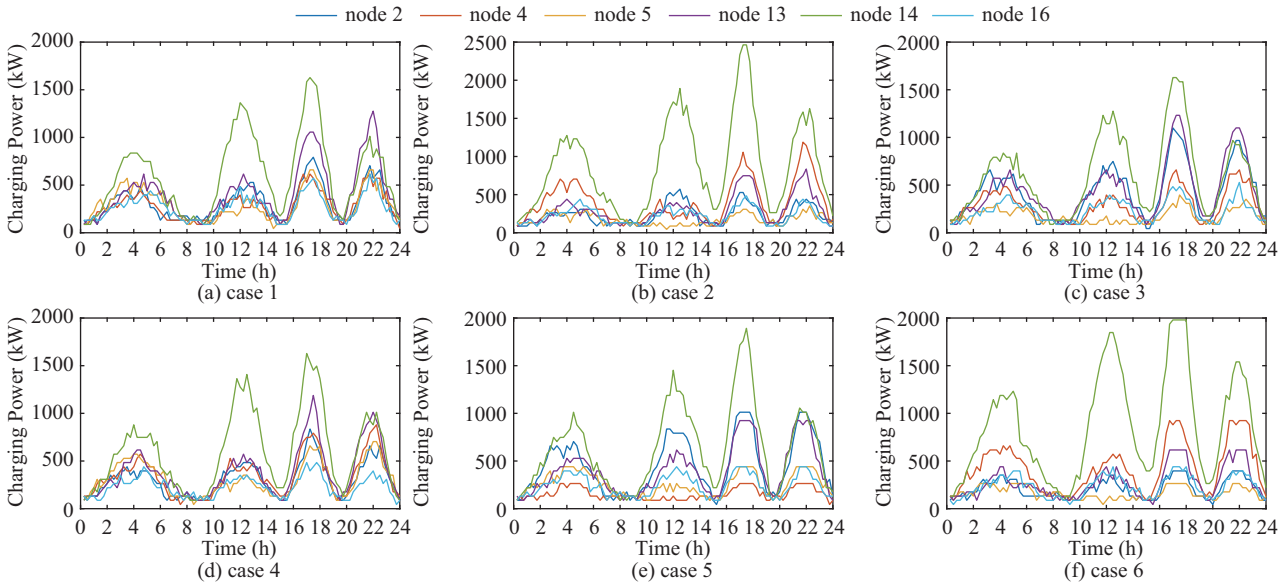

Fig. 5. Daily charging load profiles in case 1–6.

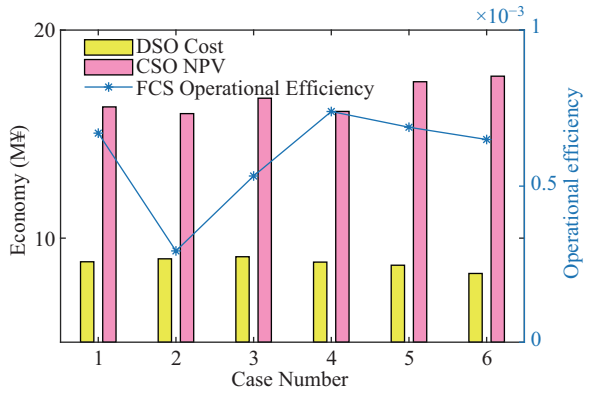

Fig. 6. Objective results of all cases.

As for the charging demands and planning results in cases 3 and 4, where the objectives focus on only the NPV or the operational efficiency of CSO, the results are different from case 1. Node 14 is the last node to capture EV flow in the three cases, and its charging peaks in cases 3 and 4, shown in Fig. 5(c) and (d), are 1.628 MW and 1540 MW, respectively. Node 13 is set to capture EV flow, being the first in the three cases, which indicates that node 13 performs well in both economic performance and operational efficiency. While the peak load and the sizes of FCS in node 2 in case 3 are higher than those in case 4, which shows a larger FCS in node 2 and is more profitable. Comparing the results of the three cases with different objectives from Table IV and Fig. 6, it is shown that case 3 has the best economic performance with a NPV 16.726 M¥, case 4 has the best operational efficiency 7.49×10^{-4}, while case 1 has the best comprehensive properties with a NPV 16.308 M¥, operational efficiency 7.36×10^{-4} and average SA 9.91%. Considering the profits and the operations for FCSs, case 1 seems to be the best choice. It is worth mentioning that the capturing flow of the nodes with high land prices in the SCFCLM is less than that in FCLM. Thus, the FCSs at the nodes with higher prices will reduce their capacities, and so the planning scheme of FCSs for SCFCLM is more practical.

C. Chance Constrained Approach and Analysis

We investigate the impact of the confidence levels ε_1 and ε_2 on the performances of planning strategies of DNEP and FCSs. Case 1 is extended and the deterministic bi-level planning is transformed into a stochastic model using the proposed chance constrained formulation as shown in (38)–(39). $\varepsilon_1 = \varepsilon_2 = 95\%$ in Case 5 and $\varepsilon_1 = \varepsilon_2 = 90\%$ in Case 6 should guarantee the satisfaction rates of constraints of the feeder capacities and node voltage amplitudes, which are 95% and 90%, respectively.

The charging demands of case 5 and case 6 are shown in Fig. 5(e) and (f), respectively. The peak loads of node 14 are 1.892 MW and 1.980 MW in case 5 and case 6 respectively, which are more than that in case 1. It means that the increasing of confidence promotes the enlargement of FCS in node 14, which appeals to more PEVs to get charged and results in the increscent peak load of FCS in node 14. With the relaxation increase of the operational constraints, the differences between peak load and off-peak load increase and subsequently results in the decrease of operational efficiency as shown in Fig. 6. While the total costs of DNEP in case 5 and case 6 are lower than the cost of the deterministic model (Case 1), and are reduced to 0.166 M¥ and 0.562 M¥, respectively. This fact is because the grid planning with the relaxed constraints requires fewer capacities of feeders and substations. Thus, the power system is able to accept the larger FCSs, which is beneficial to the CSO. The NPV of CSO in case 5 is 1.209 M¥ higher than that of case 1; and in case 6, the NPV is 1.476 M¥ higher than that of case 1.

Then we evaluate the three cases in terms of nodal voltage as shown in Fig. 7 and feeder capacity constraints in Table V. It can be observed that the strategy of case 1 effectively limits the nodal voltages within the feasible range. However, for both case 5 and case 6, some nodes violate the lower bound due to the larger FCSs, which is allowed by the relaxed constrained power grid. On the other hand, Table V shows the power network planning strategies with deterministic (case 1) and stochastic approaches (case 5 and 6). The number of upgraded feeders decreases with the confidence increase. And 2 and 4 feeders violate the upper bound of capacity constraints in case 5 and case 6, respectively.

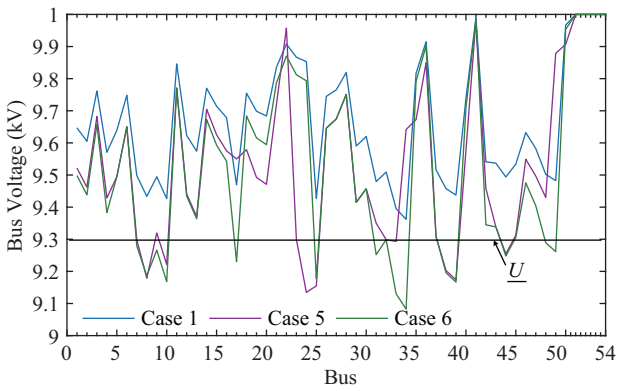

Fig. 7. Voltage results at peak load case 1, 5, and 6.

TABLE V
DIFFERENCES OF POWER NETWORK EXPANSION IN DETERMINISTIC AND STOCHASTIC PLANNING APPROACHES

Case	Feeder Construction	Feeder Update	Substation Update	Feeder Capacity Violation
1	9-17, 22-23, 23-24, 34-33, 48-49	1-9, 3-4, 35-36	53	none
5	9-17, 9-23, 24-25, 34-35, 49-50	14-46	53	11-12, 11-52
6	17-18, 9-23, 23-24, 34-35, 49-50	none	53	11-12, 11-52, 28-53, 35-36

Of course, the reliability and security of the power system will be challenged by the uncertainties of increasing charging load. Considering the acceptability of two systems, decision makers should carefully select proper confidence levels, by which the security and economic performance of the system can be balanced.

VII. Conclusion

This paper provides a stochastic bi-level method for the coordinated planning of the FCSs and distribution network expansion. An SCFCLM optimizing capturing flow sequence using a two-stage model considering maximum captured EV flow, profit and service efficiency of the CSO is proposed to improve the rationality of the FCSs planning schemes. The probability distributions of PEV charging behaviors are taken into account in the fast charging demand estimation. To improve the economic performance of transformative construction in the distribution network, chance constrained programming is used in the DENP. In the case studies, six cases are compared, which demonstrate that: 1) Compared with the case adopting traditional FCLM, the proposed SCFCLM can reasonably allocate the sizes among the candidate FCSs by optimizing the capture sequence, yielding both economic planning and efficient operations. 2) According to the bi-level framework and considering the proposed SCFCLM, the proposed method brings a more balanced charging demand distribution, which alleviates the stress on the power grid while not sacrificing much of the economic outcome through proper coordination. 3) By introducing the confidence levels into the chance constrained programming, our proposed method can consider the expected security of the system as well as reality implications on the different nature of loads.

Our ongoing study is to evaluate the planning of FCSs when multiple CSOs compete with each other for their share of the fast charging facilities investment market in an urban transportation area. The model to describe the competition relationships of CSOs will be the research focus.

References

[1] X. Q. Zhang, "The Development Trend of and Suggestions for China's Hydrogen Energy Industry", *Engineering*, vol. 7, pp. 719–721, Jun. 2021.

[2] A. Ahmad, M. S. Alam, and R. Chabaan, "A comprehensive review of wireless charging technologies for electric vehicles," *IEEE Transactions on Transportation Electrification*, vol. 4, no. 1, pp. 38–63, Mar. 2018.

[3] H. C. Zhang, Z. C. Hu, Z. W. Xu, and Y. H. Song, "An integrated planning framework for different types of PEV charging facilities in urban area," *IEEE Transactions on Smart Grid*, vol. 7, no. 5, pp. 2273–2284, Sep. 2016.

[4] X. Q. Huang, J. Chen, H. Yang, Y. J. Cao, W. D. Guan, and B. C. Huang, "Economic planning approach for electric vehicle charging stations integrating traffic and power grid constraints," *IET Generation, Transmission & Distribution*, vol. 12, no. 17, pp. 3925–3934, Sep. 2018.

[5] M. J. Hodgson, "A flow-capturing location-allocation model," *Geographical Analysis*, vol. 22, no. 3, pp. 270–279, Jul. 1990.

[6] W. F. Yao, J. H. Zhao, F. S. Wen, Z. Y. Dong, Y. S. Xue, Y. Xu, and K. Meng, "A multi-objective collaborative planning strategy for integrated power distribution and electric vehicle charging systems," *IEEE Transactions on Power Systems*, vol. 29, no. 4, pp. 1811–1821, Jul. 2014.

[7] A. Shukla, K. Verma, and R. Kumar, "Multi-objective synergistic planning of EV fast-charging stations in the distribution system coupled with the transportation network," *IET Generation, Transmission & Distribution*, vol. 13, no. 15, pp. 3421–3432, Aug. 2019.

[8] J. Yang, M. Zhang, and X. Chen, "A class of the flow capturing location-allocation model with service radius," *System Engineering: Theory and Practice*, vol. 26, no. 1, pp. 117–122, Jan. 2006.

[9] M. Kuby and S. Lim, "The flow-refueling location problem for alternative-fuel vehicles," *Socio-Economic Planning Sciences*, vol. 39, no. 2, pp. 125–145, Jun. 2005.

[10] H. C. Zhang, S. J. Moura, Z. C. Hu, and Y. H. Song, "PEV fast-charging station siting and sizing on coupled transportation and power networks," *IEEE Transactions on Smart Grid*, vol. 9, no. 4, pp. 2595–2605, Jul. 2018.

[11] H. C. Zhang, S. J. Moura, Z. C. Hu, W. Qi, and Y. H. Song, "A second-order cone programming model for planning PEV fast-charging stations," *IEEE Transactions on Power Systems*, vol. 33, no. 3, pp. 2763–2777, May 2018.

[12] B. Zhou, G. Chen, Q. K. Song, and Z. T. Dong, "Robust chance-constrained programming approach for the planning of fast-charging stations in electrified transportation networks," *Applied Energy*, vol. 262, pp. 114480, Mar. 2020.

[13] H. Y. Mak, Y. Rong, and Z. J. M. Shen, "Infrastructure planning for electric vehicles with battery swapping," *Management Science*, vol. 59, no. 7, pp. 1557–1575, Apr. 2013.

[14] P. S. You and Y. C. Hsieh, "A hybrid heuristic approach to the problem of the location of vehicle charging stations," *Computers & Industrial Engineering*, vol. 70, pp. 195–204, Apr. 2014.

[15] Y. X. Liu, H. Q. Dong, S. Y. Wang, M. X. Lan, M. Zeng, S. Zhang, M. Yang, and S. Yin, "An optimization approach considering user utility for the PV-storage charging station planning process," *Processes*, vol. 8, no. 1, pp. 83, Jan. 2020.

[16] R. Z. Yang and Q. N. Cao, "Time-satisfaction of data series based on computer original genetic algorithm gradually covers the location and algorithm of electric vehicle charging station," *Journal of Intelligent & Fuzzy Systems*, vol. 37, no. 5, pp. 5993–6001, Nov. 2019.

[17] M. Moradijoz, M. P. Moghaddam, and M. R. Haghifam, "A flexible distribution system expansion planning model: a dynamic Bi-Level approach," *IEEE Transactions on Smart Grid*, vol. 9, no. 6, pp. 5867–5877, Nov. 2018.

[18] M. H. Amini, M. P. Moghaddam, and O. Karabasoglu, "Simultaneous allocation of electric vehicles' parking lots and distributed renewable resources in smart power distribution network," *Sustainable Cities and Society*, vol. 28, pp. 332–342, Jan. 2017.

[19] Y. Xiang, J. Y. Liu, R. Li, F. R. Li, C. H. Gu, and S. Y. Tang, "Economic planning of electric vehicle charging stations considering traffic constraints and load profile templates," *Applied Energy*, vol. 178, pp. 647–659, Sep. 2016.

[20] Y. C. Zheng, Z. Y. Shao, Y. M. Zhang, and L. N. Jian, "A systematic methodology for mid-and-long term electric vehicle charging load forecasting: the case study of Shenzhen, China," *Sustainable Cities and Society*, vol. 56, pp. 102084, May 2020.

[21] S. Y. Sun, Q. Yang, J. Ma, A. J. Ferré, and W. J. Yan, "Hierarchical planning of PEV charging facilities and DGs under transportation-power network couplings," *Renewable Energy*, vol. 150, pp. 356–369, May 2020.

[22] S. M. Moghaddas-Tafreshi, M. Jafari, S. Moheni, and S. Kelly, "Optimal operation of an energy hub considering the uncertainty associated with the power consumption of plug-in hybrid electric vehicles using information gap decision theory," *International Journal of Electrical Power & Energy Systems*, vol. 112, pp. 92–108, Nov. 2019.

[23] T. Zeng, H. C. Zhang, and S. Moura, "Solving overstay and stochasticity in PEV charging station planning with real data," *IEEE Transactions on Industrial Informatics*, vol. 16, no. 5, pp. 3504–3514, May 2020.

[24] N. B. Arias, A. Tabares, J. F. Franco, M. Lavorato, and R. Romero, "Robust joint expansion planning of electrical distribution systems and EV charging stations," *IEEE Transactions on Sustainable Energy*, vol. 9, no. 2, pp. 884–894, Apr. 2018.

[25] A. Abdalrahman and W. H. Zhang, "PEV charging infrastructure siting based on spatial–temporal traffic flow distribution," *IEEE Transactions on Smart Grid*, vol. 10, no. 6, pp. 6115–6125, Nov. 2019.

[26] S. Zeynali, N. Rostami, M. R. Feyzi, and B. Mohammadi-Ivatloo, "Multi-objective optimal planning of wind distributed generation considering uncertainty and different penetration level of plug-in electric vehicles," *Sustainable Cities and Society*, vol. 62, pp. 102401, Nov. 2020.

[27] C. Olson, E. Lee, and B. Langdon, (2005). "White Paper on Ion Beam Transport for ICF: Issues, R&D Need, and Tri-Lab Plans," [Online]: Available: https://escholarship.org/uc/item/5zs0k05p.

[28] W. S. Jung, F. Z. Wang, and H. E. Stanley, "Gravity model in the Korean highway," *Europhysics Letters*, vol. 81, no. 4, pp. 48005, Feb. 2008.

[29] L. Zhang, R. Y. Huo, G. W. Cai, K. L. Hai, L. Lyu, and P. Wang, "A joint planning method of charging piles and charging-battery swapping stations considering spatial-temporal distribution of electric vehicles," *CSEE Journal of Power and Energy Systems*. [Online], Available: 10.17775/CSEEJPES.2021.05780.

[30] R. A. Jabr, R. Singh, and B. C. Pal, "Minimum loss network reconfiguration using mixed-integer convex programming," *IEEE Transactions on Power Systems*, vol. 27, no. 2, pp. 1106–1115, May 2012.
[31] S. Y. Zhou, Y. X. Zhang, Z. Wu, W. Gu, P. Yu, J. Q. Du, and X. E. Luo, "Planning and real-time pricing of EV charging stations considering social welfare and profitability balance," *CSEE Journal of Power and Energy Systems*, vol. 7, no. 6, pp. 1289–1301, Nov. 2021.
[32] Nimabm. (Feb. 2018). Adaptive genetic algorithm based on fuzzy rules. [Online], Available: https://github.com/nimabm/ADAPTIVE-GENETIC-ALGORITHM-BASED-ON-FUZZY-RULES

Shiqu Xiao received a B.S. degree in Mechatronic Engineering from Nanjing Forestry University, Nanjing, China, in 2019. He is currently pursuing an M.S. degree in Electrical Engineering at Xihua University, Chengdu, China. His main research interests are transportation electrification and distribution power system planning.

Xia Lei received a Ph.D. degree in Electrical Engineering from Sichuan University. She is currently a Professor in the School of Electrical Engineering and Electronic Information at Xihua University. Her research interests are the optimal operation of electrical systems with renewable energy and power markets.

Tao Huang received a Ph.D. degree from Politecnico di Torino, Torino, Italy. He is currently working as a Ph.D. student supervisor in the Department of Energy at Politecnico di Torino. His research interests include critical infrastructure protection, vulnerability detection and resilience enhancement, electricity markets, and smart grids.

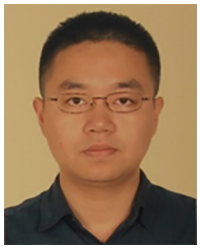

Xiang Wang received a B.S. degree and a Ph.D. degree in Electrical Engineering from Southwest Jiaotong University (SWJTU), Chengdu, China, in 2010 and 2019, respectively. He is currently a Lecturer at Xihua university since 2020. His research interests include electric vehicle to grid interaction stability and reliability, the electric vehicle providing ancillary services for power system, as well as integrated energy systems and demand response.